

# A Laboratory Investigation of Enhanced Gas Recovery by CO<sub>2</sub> Injection

Chris Jones<sup>1,\*</sup>, Mike Spearing<sup>1</sup>, Maynard Marrion<sup>1</sup>, Arief Maulana<sup>2</sup> and Frans Silitonga<sup>2</sup>

<sup>1</sup> BP, Sunbury on Thames, United Kingdom

<sup>2</sup> BP, Jakarta, Indonesia

**Abstract** A core flood study was undertaken to measure dynamic displacement characteristics of CO<sub>2</sub>, CH<sub>4</sub> and brine as part of a feasibility study for a proposed carbon capture, utilisation and storage (CCUS) development. The planned project involves separation of CO<sub>2</sub> from reservoir gas and its reinjection into the reservoir. This was both to sequester the CO<sub>2</sub> and to recover trapped hydrocarbon gas from the underlying paleo residual gas zone. Key parameters measured in order to model the enhanced gas recovery (EGR) process included drainage and imbibition relative permeabilities, trapped gas saturations and hydrocarbon gas recovery efficiency. To properly reproduce the miscibility conditions for the EGR process, equilibrium fluids at reservoir conditions were used. Reservoir conditions were also used as the wetting character of CO<sub>2</sub>, which was in the super-critical state at the test conditions, was uncertain from the literature. Strong water wet conditions would favour water blocking of the trapped methane to the injected CO<sub>2</sub>, whereas partial CO<sub>2</sub> wetting, as some literature suggests, would imply less water blocking. As well as characterising the EGR efficiency, trapped methane and trapped CO<sub>2</sub> were measured during the SCAL program. Differences in Land Correlations for these fluids were observed for a given rock type. Comparison of trapped CO<sub>2</sub> at reservoir conditions to trapped N<sub>2</sub> at ambient conditions is discussed. The trapped gas saturation to methane and to CO<sub>2</sub> was modelled by digital rock physics and implied the CO<sub>2</sub> was partially wetting.

## 1 Introduction

One possible solution to reduce the effects of anthropogenic CO<sub>2</sub> release is sequestration into the geological subsurface [1], including depleted oil or gas fields [2]. If captured CO<sub>2</sub> is injected into a partially produced hydrocarbon gas reservoir it can provide pressure maintenance, prolonging production, and is referred to as enhanced gas recovery (EGR) [3,4].

Many producing hydrocarbon reservoirs sit above so-called paleo residual oil or gas zones (ROZ / RGZ) [5]. Hydrocarbons in these zones do not flow due to being comprised of non-continuous ganglia of hydrocarbon surrounded by a continuous brine phase at the pore scale. For this reason, residual oil and gas zones are fundamentally different to main pay zones and often uneconomic to produce [6,7,8]. There are different causes of ROZ/RGZs: regional tilting of a basin, leakage followed by healing of reservoir seal and changing hydrodynamics in the underlying aquifer [5]. The case in point for this study is due to the first, tilting of structure over geological time, and can therefore be referred to as a Paleo Residual Gas (PRG) Zone.

This laboratory study aimed to provide relative permeability, trapped gas saturation and displacement efficiency of paleo residual hydrocarbon gas to evaluate the engineering and economic benefits for two principal CCUS options for a sandstone dry gas reservoir; injection of CO<sub>2</sub> into the gas leg or into the aquifer beneath the main pay which

contained paleo residual gas. Comparisons will also be drawn with injecting CO<sub>2</sub> into an entirely brine filled aquifer.

## 2 Materials and Methods

All corefloods were conducted using the unsteady state method [9] using two different coreflood rigs and a series of either equilibrium synthetic reservoir fluids or a simplified nitrogen / brine system as described below.

### 2.1. Fluid and Core Preparations

Synthetic brine was made to match the reservoir connate water with a TDS of 37,500 ppm. To improve in-situ saturation monitoring (ISSM) a second brine was used which was doped with 50 g/L sodium iodide [10], replacing some of the sodium chloride in the undoped brine to give a TDS of 68,500 ppm. The ionic makeup of the brines used for all experiments is summarized below in Table 1.

\* Corresponding author: [christopher.jones2@uk.bp.com](mailto:christopher.jones2@uk.bp.com)

**Table 1.** Compositions of undoped and sodium iodide doped brines

Ion	Undoped Brine mg/L	Doped Brine mg/L
Sodium	13711	14087
Calcium	171	171
Potassium	804	804
Magnesium	34	34
Carbonate (CO <sub>3</sub> )	60	60
Chloride	22785	10959
Iodide	0	42331
<b>TDS (ppm)</b>	<b>37,565</b>	<b>68,447</b>

Live brines for the reservoir condition corefloods were made by contacting the dead fluid with either CH<sub>4</sub> or CO<sub>2</sub> at test conditions until saturated. At the reservoir condition pore pressure of 3000 psi and temperature 90 °C the CO<sub>2</sub> was in the supercritical state. For the ambient condition tests equilibrium fluids were made in the coreflood rig by contacting nitrogen gas and brine phases as described in the equipment description below. Viscosities and densities for the fluids used in the experiments are summarized below in Table 2.

**Table 2.** Properties of fluids used in corefloods at test conditions

Reservoir condition tests (90 °C, 3000 Psig)	Density (g/cc)	Viscosity (cP)
Doped brine	1.021	0.372
CO <sub>2</sub>	0.553	0.042
CH <sub>4</sub>	0.117	0.018
Ambient condition tests (20 °C, 250 Psig)		
Doped Brine	1.047	1.084
N <sub>2</sub>	0.020	0.018

The work reported was part of a larger special core analysis (SCAL) study which used several cores from various locations in the field, including one from the PRG zone. Cores varied in age, only some were wax preserved and some had been 2/3 slabbed. The PRG core was unpreserved and 20 years old. Log evidence suggested that there was little difference in reservoir quality between gas leg, water leg, crestal or flank core and so it was decided that it was not necessary to use such old, unpreserved core to represent the PRG zone. After CT scanning of all whole core pieces a total of 43 plugs were cut under brine from four different cored wells covering 4 rock types (RT). In order to understand whether drying out of some of the unpreserved cores had caused damage, X-Ray diffraction (XRD) of crushed samples and scanning electron microscopy (SEM) of freshly fractured surfaces was carried out. XRD data suggested most samples contained ~0.1 wt% Halite, with one containing 0.3 wt%. In this later sample, SEM images of the fracture surface showed small salt crystals, but they did not appear to have disrupted

the clay material present and could reasonably be expected to dissolve into brine upon re-saturation. Based on these investigations it was concluded that the drying had not adversely affected the available samples. Consequently the plugs used in the work presented here were all cut from a 2/3 slabbed whole core from the gas leg as this core best matched the porosity and permeability of the target rock type. This study concerns measurements on one volumetrically dominant RT.

## 2.2. Ambient condition coreflood rig

The ambient condition corefloods were performed at a pore pressure of 250 psi, confining pressure of 1000 psi and ambient lab temperature. A continuous supply of humidified nitrogen was produced by flowing nitrogen through deionised water before it entered the core. Nitrogen saturated brine was flowed to the vertically mounted core from a dedicated live brine makeup vessel using a Quizix QX pump.

The ISSM system consisted of 12 pairs of Americium 241 sources and scintillation detectors along the length of the core [11]. Hydrostatic overburden was applied with deionised water.

Constant differential pressure (DP) nitrogen floods were performed by off-setting inlet and outlet mass flow controllers whilst brine floods used the Quizix pump in constant rate mode. DP across the core was measured independently by dedicated differential pressure cells. See Figure 1.

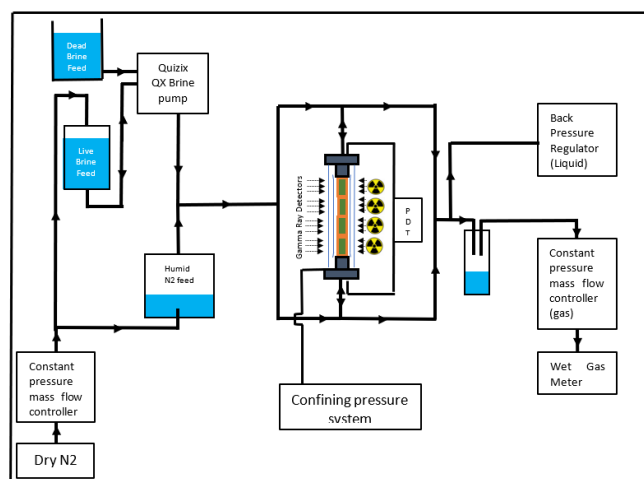


**Fig. 1.** Ambient condition nitrogen / brine coreflood rig

## 2.3. Reservoir condition coreflood rig

All reservoir condition corefloods were performed at the predicted future reservoir pore pressure of 3000 psi, confining pressure of 8900 psi and temperature 90 °C. The coreflood rig included a visual separator immediately downstream of the vertically orientated coreholder, used to measure production at pore pressure. This was housed inside an oven along with the carbon fibre coreholder and fluid delivery piston vessels to maintain temperature equilibrium. Fluid from the separator flowed into a dip-tube vessel from where only live brine fluid flashed across the back pressure regulator

(BPR). An ISSM system very similar to that on the ambient condition coreflood rig was used. Confining pressure was applied with deionised water held at pressure by a gas buffer system. See Figure 2.

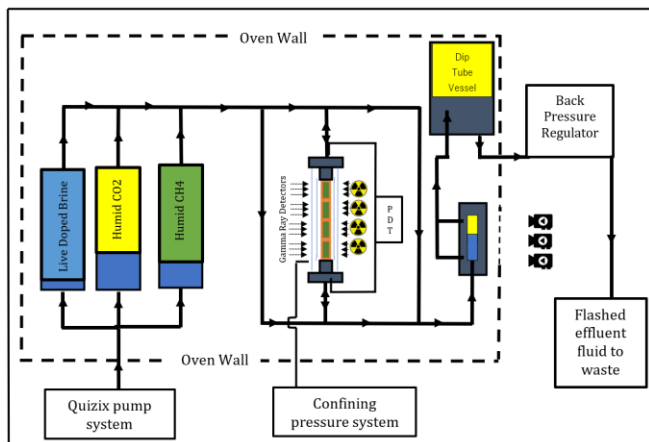


**Fig. 2.** Reservoir Condition Coreflood setup with separator at pore pressure

Effluent flow from the outlet end of the core could also be routed directly to a second BPR after which a low pressure separator system was located. This consisted of a pair of switchable CO<sub>2</sub> purged liquid dropout cells used to collect brine effluent and a twin piston gasometer which collected produced gas for subsequent sampling. Where gas samples were not needed, gas flow could be directed to a logged wet gas meter, as shown in Figure 3.

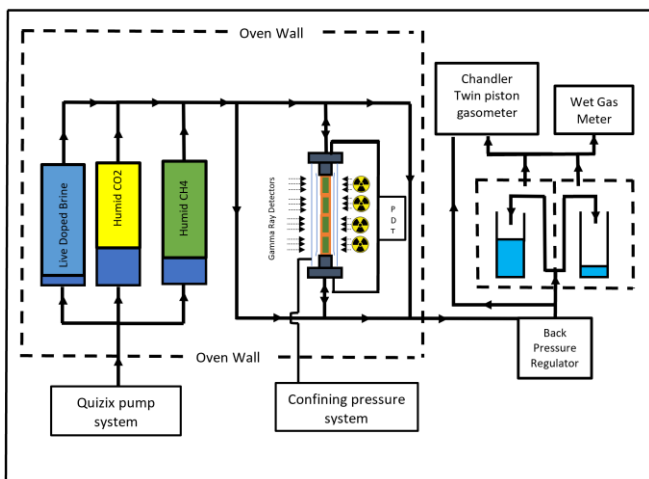


**Fig. 3.** Reservoir Condition Coreflood with effluent from core flashed to low pressure separator and gasometer

#### 2.4. Gas sampling from reservoir condition coreflood tests

Flashed gas samples from the reservoir condition EGR and dispersion tests flowed either from the low pressure separator or directly to the gasometer as shown in Figure 3. The entire sample collection system was purged with CO<sub>2</sub> gas each time a sample was taken. Gas samples were transferred to Tedlar sample bags for Gas Chromatography (GC) analysis, using CO<sub>2</sub> as the carrier gas.

### 3 Experimental Procedures

Whole cores used for the study were received in a 2/3 slabbed non-preserved state and CT scanned to select the most representative plugging sites. Plugs were cut under brine before being cleaned by flowing cycles of methanol and toluene until effluent was observed to be clear. They were saturated in brine ( $S_w = 1$ ) and their permeability measured at multiple flow rates, followed by pore volume by miscible dispersion to sodium iodide doped brine (doped brine). Plugs were either desaturated to an initial water saturation ( $S_{wi}$ ) via porous plate or loaded directly into the coreflood rigs at  $S_w = 1$  as applicable to the following test.

#### 3.1 Ambient condition brine displacing nitrogen corefloods

Single core plugs were prepared to  $S_{wi}$  using the porous plate technique to ensure uniform water saturation. Once at  $S_{wi}$ , selected core plugs were mounted inside Viton rubber sleeves and hydrostatic overburden applied to the coreholder using deionised water.

Effective gas permeability at  $S_{wi}$  was measured at four differential pressures using humidified nitrogen. Coreholder bypass lines were then swept with nitrogen saturated brine before the gravity stable imbibition floods were started at between 4 to 10 ml/hr using the Quizix pump. A series of corefloods on other rocktypes for the same study showed that  $S_{gt}$  did not vary with changes in flow rate of this order. These continued for 2 pore volumes (PV) injected or less if ISSM and DP indicated no further saturation change. The brine permeability at trapped gas saturation was measured by stepping down the brine flow rate.

The plugs were then degassed by flowing dead brine and cycling back pressure. Dead brine was displaced with nitrogen saturated brine, the ISSM calibration recorded and absolute permeability to brine ( $K_w$ ) measured.

To reach  $S_g = 1$  with humidified nitrogen, the core was flushed with 5 PV each of methanol, toluene and pentane before the pore pressure was removed and the pentane vapourised with dry nitrogen. Pore pressure was then reapplied and several PVs of humidified nitrogen flowed at four different DP's to measure  $K_g$  and record the  $S_g = 1$  ISSM calibration.

#### 3.2 Reservoir condition coreflood $K_r$ Tests

Three plugs were chosen with well-matched permeability and porosity, and built into a composite with the highest permeability plug at the bottom. This was to minimise retention of brine at the outlet end with respect to the primary drainage flood. The composite was heat-shrunk, wrapped in aluminium foil material before a Viton rubber sleeve was fitted. The composite was loaded into the coreflood rig at  $S_w = 1$  with dead undoped brine and taken to test conditions. Total pore volume was measured by brine dispersion to dead doped brine before the composite was saturated in live doped brine (doped brine saturated with CO<sub>2</sub> at test conditions) to provide ISSM calibration data for  $S_w = 1$  saturation.

Bypass lines around the coreholder were flushed with humidified CO<sub>2</sub> before a gravity stable primary drainage flood was performed at 10mL/h whilst saturation was

monitored using both the separator and ISSM system for 20 PVs of injection. Bump floods at 40 then 400 ml/hr were then performed for 20 and 30 PV's respectively to investigate capillary end effects. CO<sub>2</sub> permeabilities were measured at four reducing rates at the end of each flood rate.

Core bypass lines were then flushed with CO<sub>2</sub> saturated brine before a gravity stable imbibition flood was performed at 4ml/h, and continued until free gas production stopped. The endpoint brine permeability was measured at four reducing rates.

In order to obtain a 100% phase ISSM calibration for humidified CO<sub>2</sub>, dead brine was flowed through the composite to dissolve all gas until DP and ISSM were stable. The dead brine was miscibly displaced with the sequence of methanol, toluene, pentane, dry CO<sub>2</sub> and finally humidified CO<sub>2</sub>. CO<sub>2</sub> permeability was also measured at this point.

Finally, the composite was degassed using dead doped brine again until Sw=1 was reached and the rig was brought down from reservoir conditions before unloading.

### 3.3 Reservoir condition coreflood EGR tests

The composite from the kr coreflood test was deconstructed and the three plugs individually desaturated from 100% doped brine to Swi using the porous plate method [9]. The composite was rebuilt in an identical way to the kr coreflood.

After reloading into the coreflood rig, reservoir conditions were applied and nitrogen was displaced with humidified methane. Effective permeability to gas (k<sub>eg</sub>) at Swi was measured at four rates. The rig was configured so that effluent from the core flowed directly to a BPR and was collected in the CO<sub>2</sub> purged twin piston gasometer for sampling and subsequent GC analysis.

Bypass lines were swept with humidified CO<sub>2</sub> to minimise dead volume corrections in the subsequent gas chromatographic (GC) analysis of the collected CH<sub>4</sub>. A gravity stable miscible dispersion with humidified CO<sub>2</sub> invading to displace humidified CH<sub>4</sub> was carried out with effluent collected into sample bags for GC analysis. CO<sub>2</sub> was then displaced back to humidified methane.

The rig was re-configured to use the high pressure separator before the BPR and core bypass lines were flushed with methane saturated brine. A 4 ml/hr gravity stable imbibition to S<sub>gt</sub>(CH<sub>4</sub>) was carried out until ISSM and DP were stable and production of free gas had ceased. Effective permeability to brine (k<sub>ew</sub>) at S<sub>gt</sub> was measured and the core was now in the saturation state representing the paleo residual hydrocarbon zone.

In preparation for the EGR flood the rig was setup with the low pressure separator after the BPR where liquid was collected and downstream of this gas flow could be directed to either the gasometer or wet gas meter. Bypasses were swept with humidified CO<sub>2</sub> to replace brine in the dead volumes.

The EGR CO<sub>2</sub> flood was performed downwards (gravity stable with respect to the continuous brine phase in the core) at 4 ml/hr. The flood continued until brine production had ceased and GC analysis indicated that only CO<sub>2</sub> was being produced.

The core was flooded with dead brine to degas followed by a dispersion to dead doped brine to confirm total pore

volume. CO<sub>2</sub> and separately CH<sub>4</sub> saturated brine permeabilities and ISSM calibrations followed.

The composite was miscibly displaced to 100 % CH<sub>4</sub> using the solvent sequence describe above in Section 3.2. The final dispersion of humidified CO<sub>2</sub> displacing humidified CH<sub>4</sub> at S<sub>g</sub> = 1 was carried out with gas samples collected for GC analysis. This was done to provide a comparison to the EGR coreflood where CO<sub>2</sub> miscibly displaced CH<sub>4</sub> but in the presence of a continuous water phase. Remaining 100% phase ISSM calibrations and permeabilities were measured.

## 4 Results

### 4.1 Ambient brine displacing nitrogen corefloods

Effective gas permeabilities at Swi were measured as 178.3 mD and 92.8 mD for the two individual corefloods.. ISSM derived Swi were 0.09 and 0.13 PV respectively. The trapped gas saturations from ISSM were measured at 0.49 and 0.50 PV. S<sub>gi</sub> vs. S<sub>gt</sub> data fitted reasonably on a single Land function [12] as shown below in Figure 14.

Basic properties of the two individual plugs used for the ambient condition are summarised below in Table 3.

**Table 3.** Properties of individual plugs used for ambient condition corefloods

	Length (cm)	CSA (cm <sup>3</sup> )	PV (cm <sup>3</sup> )	Porosity (frac)	Kw@ Sw=1 (mD)
Plug 1	7.63	10.98	11.82	0.141	175.9
Plug 2	7.65	11.27	12.03	0.135	66.1

### 4.2 Reservoir condition kr core floods

Basic properties of the composite used for the reservoir condition corefloods are summarised below in Table 4.

**Table 4.** Properties of composite of three plugs used for reservoir condition corefloods.

Length (cm)	CSA (cm <sup>3</sup> )	PV (cm <sup>3</sup> )	Porosity (frac)	Kw@ sw=1 (mD)
22.75	11.16	33.61	0.132	122

Permeability of the composite to live brine was measured at 122 mD, slightly lower than the harmonic mean of the three individual permeabilities measured at ambient conditions, as would be expected with the increased net overburden.

The primary drainage flood was carried out initially at 10 ml/hr and breakthrough occurred after 0.29 PV's of humidified CO<sub>2</sub> had been injected (PVi). Water production continued for most of the 20 PVi of the 10 ml/hr flood until the rate of brine production became very slow and a S<sub>g</sub> = 0.45 PV was reached. This significant water production after breakthrough is expected of a draining system.. k<sub>rg</sub> at the remaining water saturation (Swr) was 0.031 relative to Kw.

Bump floods at 40 and 400 ml/hr increased  $S_g$  to 0.57 PV after a total throughput of 80 PV. At the end of the 400 ml/hr flood keg at Swr had increased to 64.2 mD which gave a  $k_{rg}$  relative to  $K_w$  of 0.53. There was good agreement with ISSM and separator data though there is evidence from both saturation measurements and the DP data that drainage was still continuing as shown in Figure 4.

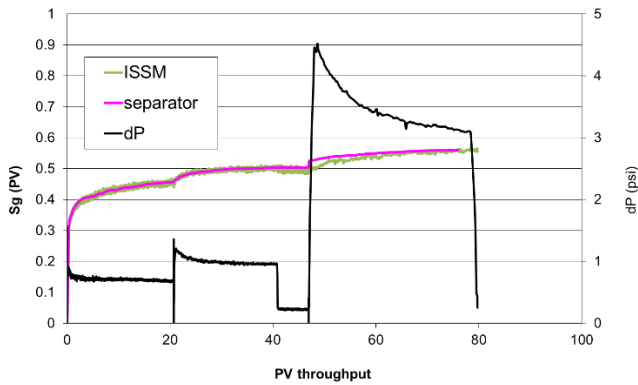


Fig. 4 Primary drainage flood saturation and DP data

Between the end of the 40 ml/hr and 400 ml/hr bumps the flow rate was reduced down to 2 ml/hr to conserve humidified  $CO_2$  whilst another batch of humidified  $CO_2$  was made and transferred into the coreflood rig.

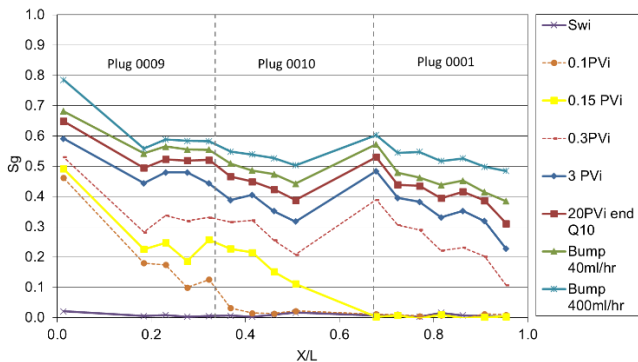


Fig. 5 ISSM saturation profiles during the primary drainage flood

Figure 5 shows ISSM saturations at varying  $PV_i$  during the 10, 40 and 400 ml/hr drainage floods. There is evidence of a butt effect between the middle and outlet plugs. This was probably caused by a capillary discontinuity across this interface and artefacts relating to this must be considered when interpreting this data. The ISSM system used for these experiments comprised of three banks of eight detectors. These were originally designed to be used with single core plugs and give full coverage along the length of a standard length core plug. When adapted for a composite of three coreplugs the individual banks of eight detectors cannot be stacked as a continuous bank of 24 due to dimensional constraints and so some undesirable gaps in the ISSM data are inevitable. ISSM information at either end of the composite was prioritised in this case which gave two

intervals with no ISSM data between 0.05-0.18 and 0.51 -0.67 fractional length. At the end of the 10 and 40 ml/hr drainage floods there is evidence of capillary retention of brine at the outlet end of the composite though this is significantly reduced during the 400 ml/hr bump flood.

Results were initially analysed using the JBN [13] method to provide  $K_r$  curves based on the raw laboratory data then using Sendra simulation software to correct for capillary pressure ( $P_c$ ) effects. Several fitting parameters were tried with LET providing the best fit for  $K_r$  data and Burdine for  $P_c$ . [14, 15]. JBN and final rock curves are shown in Figure 6.

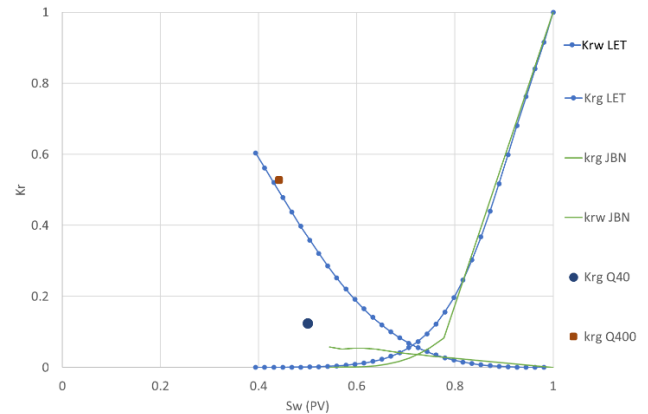


Fig. 6. Drainage relative permeability data, raw and post coreflood simulation

The brine imbibition at 4 ml/hr reached a trapped  $CO_2$  saturation of 0.34 PV after less than 1  $PV_i$ .  $kr_w$  at  $S_{gt}(CO_2)$  was 0.168 when normalised to keg at  $Sw_i$  or 0.089 when normalised to  $K_w$  at  $Sw=1$ . Due to the nature of USS corefloods only endpoint imbibition permeabilities could be measured. No post breakthrough production of  $CO_2$  was observed which is indicative of a water being the wetting phase in the system. .

### 4.3 Reservoir condition $CO_2$ EGR core flood

After ISSM calibrations were made the average  $Sw_i$  of the composite was found to be 0.12 PV with a uniform saturation along the length of the composite. Humidified methane permeability was 163 mD. The increase in permeability compared to the absolute brine permeability may be due to the  $Sw_i$  creating a less tortuous path the gas flow.

Brine imbibition to trapped methane saturation (to set up the saturation state representing the PRG) was stopped after 2  $PV_i$  as no further saturation change was observed, reaching  $S_{gt}(CH_4) = 0.545$  PV as measured by the separator in good agreement with ISSM derived data. Endpoint  $kr_w$  at  $S_{gt}(CH_4)$  was 0.0075 when normalised to keg at  $Sw_i(CH_4)$ . At this point the volume of  $CH_4$  in the core was quantified as 18.1 mL (0.54 PV) from ISSM and 18.6 mL (0.55 PV) from separator measurements

The  $CO_2$  EGR flood at 4 ml/hr lasted for 72 hours and saw 20  $PV_i$  of humidified  $CO_2$  injected downwards through the core. GC analysis of 25 gas samples showed that 19.1mL

(0.57 PV) CH<sub>4</sub> was produced, corrected to test conditions. This showed that the CO<sub>2</sub> flood recovered all available methane within experimental limits of accuracy. In addition, 4.1 mL of reservoir brine was recovered.

The mol% of CH<sub>4</sub> in the gas samples collected during the test is shown in Figure 7. The initial samples showed 100 mol% CO<sub>2</sub> as they represented production from the outlet dead volume which had been swept.

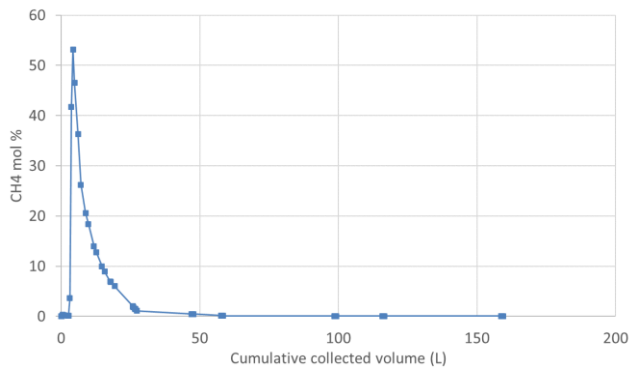


**Fig. 7.** mol % of methane in collect gas samples with outlet dead volume containing swept CO<sub>2</sub> clearly visible in first three samples.

CH<sub>4</sub> collected at atmospheric conditions and lab temperature was converted back to reservoir conditions and plotted cumulatively in Figure 8.

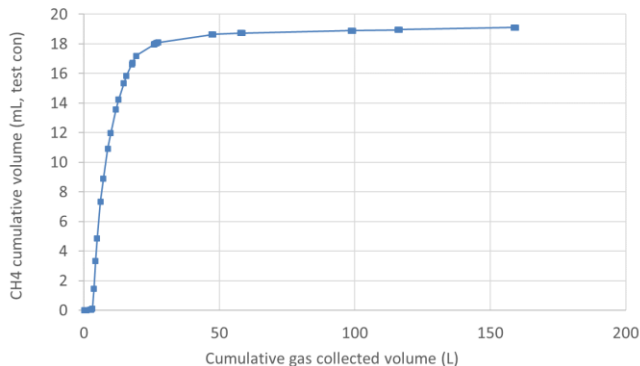


**Fig. 8.** Cumulative methane production of all of the target paleo residual gas.

The brine production means that the final CO<sub>2</sub> saturation was 0.12 PV higher when compared to the initial trapped methane saturation. Swr was 0.35 PV, see Figure 9, below. CO<sub>2</sub> permeability at Swr was 14 mD which gave kr(CO<sub>2</sub>) of 0.086 relative to keg(CH<sub>4</sub>) at Swi.

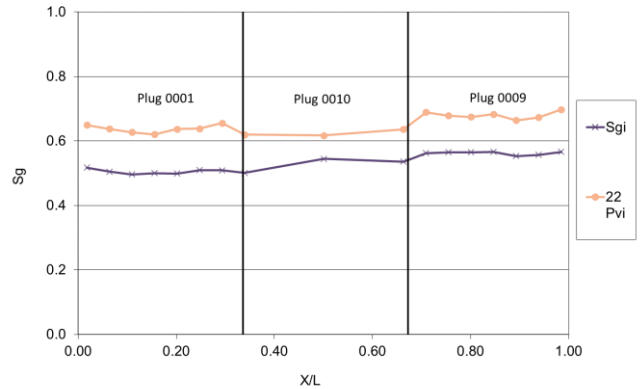


**Fig. 9.** Trapped methane concentration average of 0.53 PV in the paleo residual state and CO<sub>2</sub> concentration of 0.65 PV after the EGR flood.

The brine dispersion carried out at Sw = 1 and the CO<sub>2</sub>/CH<sub>4</sub> dispersions carried out at Sw = 0 showed only minor variations. Total pore volumes were measure at 33.6 mL in the brine system and 33.3 mL during the CO<sub>2</sub>/CH<sub>4</sub> dispersion and are shown below in Figure 10. Plots of PVi vs. invading phase concentration essentially overlaid one another in both cases. In addition, the CO<sub>2</sub>/CH<sub>4</sub> dispersion at Swi, when the gas pore volume was scaled appropriately to total pore volume the dispersion result perfectly overlaid the equivalent dispersion at Sw=0.

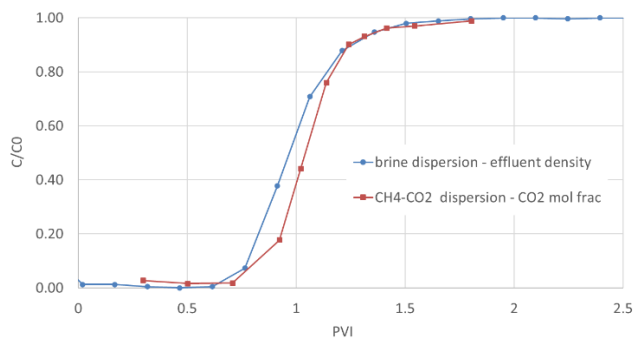


**Fig. 10.** Comparison of CH<sub>4</sub>/CO<sub>2</sub> and Brine/Brine dispersion

## 5. Discussion of results

### 5.1 Comparison of trapped gas saturations

The core plugs used for the EGR test were first individually prepared to an initial water saturation by porous plate before being built into a composite. After loading into the coreflood rig and taking to test conditions the nitrogen was displaced with humidified methane to give an initial water saturation of 0.10 to 0.14 PV uniformly distributed along the length of the composite. This was followed by the gravity stable imbibition which produced a trapped CH<sub>4</sub> saturation of 0.49-0.55 PV, with an average value of 0.53 PV. ISSM data is shown in Figure 11 below.

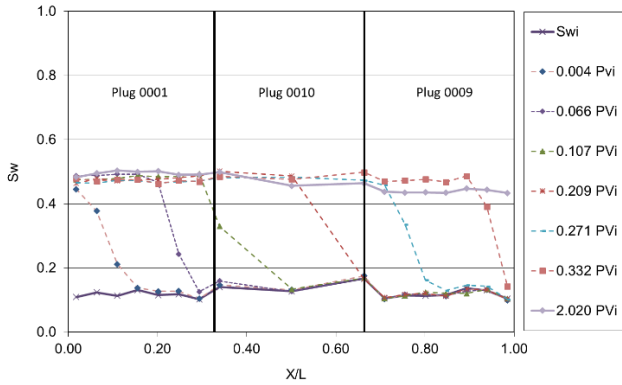


**Fig. 11.** Imbibition flood in preparation for the EGR showing trapped CH<sub>4</sub>. Uniform Swi of 0.10-0.14 PV, Uniform Sgt(CH<sub>4</sub>) of 0.49 – 0.52

In the CO<sub>2</sub>/Brine kr tests the same three plugs were loaded at Sw=1 and, after taking to reservoir conditions, the primary drainage flood was performed. This was also repeated at different flood/bump rates. These two primary drainages derived two different non-uniform Swr profiles. The two repeats of the primary drainage flood are shown as the initial water profiles in Figures 12 and 13.

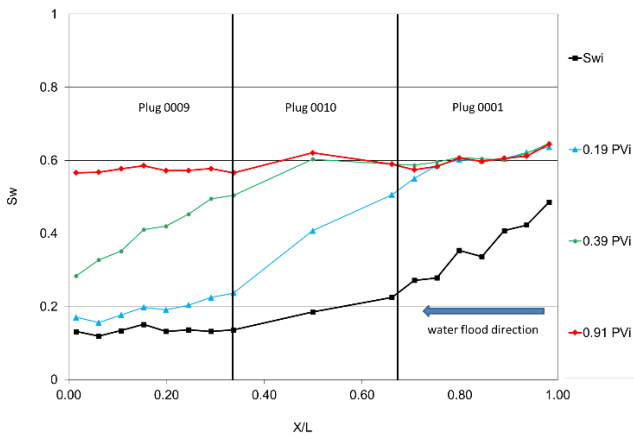


**Fig. 12.** Imbibition flood from the CO<sub>2</sub>/Brine Kr tests from a non uniform Swr after primary drainage to a more uniform Sgt(CO<sub>2</sub>) after imbibition.

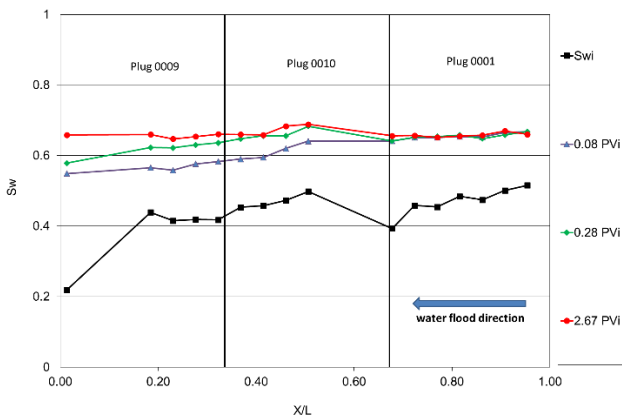


**Fig. 13.** Repeat example of the imbibition to trapped CO<sub>2</sub> from the kr coreflood tests. Identical rock and fluids but without the DP shock giving more uniform Sgi.

As shown in Figures 12 and 13, the remaining water saturations after the primary drainage floods varied significantly along the lengths of the composite due to capillary retention of brine at the outlet, and in one case, to very high rate bump. The high viscous forces in this event drove inlet saturations to very low values, comparable to those achieved on the porous plate in preparation for the EGR test. Outlet saturations however remained much higher.

Data from Figures 11-13, shown in Sw terms are collated below in Figure 14 and converted to Sg terms as Land plots [12] of Sgi vs Sgt. Sg is used for all non-brine saturations even though the CO<sub>2</sub> is in the supercritical dense phase state. Each data point represents one ISSM monitoring point along the composite.

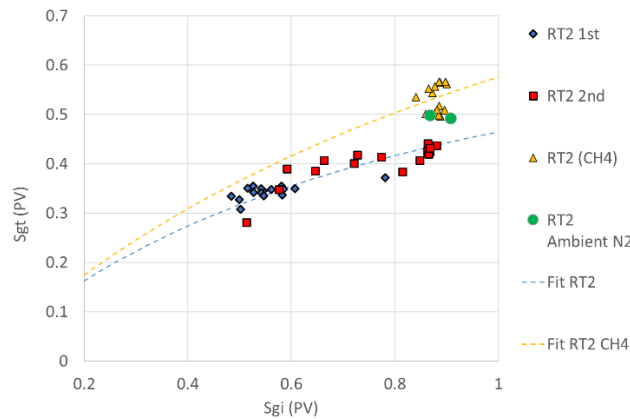


**Fig. 14.** Plot of Sgi vs Sgt for all core floods with Land fits for reservoir condition CO<sub>2</sub> / Brine and CH<sub>4</sub> / Brine data.

In Figure 14 the two repeats for the CO<sub>2</sub> / Brine system are shown by square and diamond symbols. Although these two datasets show significant variation in initial gas saturation the datapoints all sit on a single Land correlation fit with c=1.15, as would be predicted as the systems are identical though have been driven to very different Swr.

It is also clear from the plot that there is a significantly higher trapped CH<sub>4</sub> saturation (shown by the triangle symbols and yellow Land fit where c=0.74) compared to trapped CO<sub>2</sub> from very similar initial gas saturations. The CH<sub>4</sub> Sgi points are all clustered around 0.86 – 0.90 PV due to the uniformity of the Swi achieved by the porous plate method. Comparing all of these points to the cluster of ~6 ISSM points from one of the CO<sub>2</sub>/Brine floods with comparable Sgi there is a clear difference of around 0.1 PV in trapped gas saturation.

A digital rocks (DR) study was run in parallel to the SCAL tests reported here. The methodologies used for the DR analysis followed an established BP approach [16]. The DR study performed on a number of samples of the same rock type, predicted a Sgt of 0.51 - 0.52 from initial water saturations in the 0.86 - 0.90 range when a 10° contact angle between the brine and second phase was used. This is consistent with the brine being the strongly wetting phase and the second phase being entirely non wetting, as would be

expected with a gas such as methane. By changing the contact angle in the model to 70° (what would be described as an intermediate wet system) Sg<sub>t</sub>'s of 0.32 - 0.39 PV were predicted. This implies that the CO<sub>2</sub> phase in the experiments described above was partially wetting.

Corefloods performed on other rock types/ mineralogies in the same study (but not reported here) compared trapped CH<sub>4</sub> to trapped CO<sub>2</sub> at similar conditions, but showed little difference in Sg<sub>t</sub> for CO<sub>2</sub> or CH<sub>4</sub>. The difference in Sg<sub>t</sub> for CH<sub>4</sub> and CO<sub>2</sub> may be specific to this particular rock type. The other RT that did not show a material difference was of low permeability and could not be drained to a high Sg<sub>i</sub> so all datapoints were near to the convergence of the Sg<sub>i</sub> vs Sg<sub>t</sub> axes. Further work is planned to re-investigate this for better quality core.

Also plotted on Figure 14 are the two data points which represent the average Sg<sub>i</sub> vs Sg<sub>t</sub> values for the two ambient Nitrogen / Brine gas floods performed on single plugs of the same rock type. Although the test conditions are very different the Sg<sub>t</sub> reached compares well to that in the reservoir condition CH<sub>4</sub> test and suggest they are both systems with a strongly wetting brine phase and entirely non wetting gas phase.

Partial wetting of mineral surfaces by CO<sub>2</sub> in brine /CO<sub>2</sub> remains a controversial topic with no clear consensus in the literature [17-20] on whether supercritical CO<sub>2</sub> behaves like a non-wetting gas or as a partially wetting fluid. The trapped gas saturation data presented here suggest that supercritical CO<sub>2</sub> in the presence of brine at reservoir conditions may be partially wetting in some rock types. Further corefloods are ongoing to investigate this finding further.

## 5.2 Analysis of EGR flood results and comparison with miscible dispersion tests

The EGR test demonstrated complete recovery of the trapped methane. In strongly water wet oil/brine systems water blocking [21-23] can impede recovery of trapped residual oil during tertiary gas flooding. Comparison of the methane production profile from the EGR test with the CO<sub>2</sub>/CH<sub>4</sub> dispersion at Sw<sub>i</sub> are shown in Figure 15, both are dead volume corrected. The red dataset shows CO<sub>2</sub> mol fraction in the effluent from the dispersion and shows complete production after approximately 2 PV<sub>i</sub> and no brine was produced as was to be expected. The blue dataset shows the mol fraction of CH<sub>4</sub> in the gaseous effluent from the EGR flood.

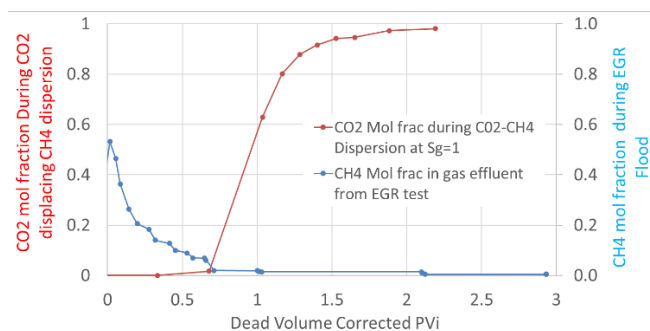


**Fig. 15.** Comparison of miscible CO<sub>2</sub>/CH<sub>4</sub> and EGR flood CH<sub>4</sub> production plotted against PV<sub>i</sub> of CO<sub>2</sub>.

Figure 15 shows co-production of CO<sub>2</sub> and CH<sub>4</sub> from the composite and that all CH<sub>4</sub> from for EGR test was produced just after 2 PV<sub>i</sub> of CO<sub>2</sub>. Brine was also produced throughout the EGR flood.

The CO<sub>2</sub>/CH<sub>4</sub> dispersion was performed to understand the nature of a simple miscible dispersion with no other fluid present. This result, along with the brine dispersion at Sw=1, provided a baseline for subsequent comparison and illustrates the contribution of rock structure on the dispersion behaviour. The repeat CO<sub>2</sub>/CH<sub>4</sub> dispersion with Sw<sub>i</sub> in place showed no significant change in behaviour due to the presence or interaction with brine at a representative irreducible saturation. Whilst the distribution and saturations of fluids in the CO<sub>2</sub>/CH<sub>4</sub> at Sw<sub>i</sub> dispersion and EGR tests were fundamentally different, complete production of the EGR target gas after a comparable through-put to the CO<sub>2</sub>/CH<sub>4</sub> dispersion at Sw<sub>i</sub> demonstrates water blocking of trapped CH<sub>4</sub> did not occur to any significant degree.

## 5.3 Comparison of remaining CO<sub>2</sub> saturation after primary and secondary drainage

Remaining water saturation after the secondary drainage EGR flood was 0.35 PV. In this flood the 20PV 4 ml/hr CO<sub>2</sub> injection produced brine and replaced all CH<sub>4</sub> which was initially present as an immobile residual phase. The CO<sub>2</sub> at Sw<sub>r</sub> was a continuous flowing phase and while brine production had ceased it was not an immobile, discontinuous phase and could have drained to a lower remaining saturation.

Comparing this result to the primary drainage from Sw=1 in the kr tests shows very different results. The initial low rate flood was at 10 ml/hr for 20 PV and reached an Sw<sub>r</sub> of 0.55 PV and was also still draining slowly. Fluid distributions are presumed to be similar to the end of the EGR test albeit with a much higher remaining water saturation.

Comparison of the above two situations has potentially significant implications for CO<sub>2</sub> use and sequestration in the subsurface. Not only could injection of CO<sub>2</sub> into a paleo residual zone produce this trapped hydrocarbon gas but it could also provide a significantly increased CO<sub>2</sub> storage capacity when compared to injecting into a solely brine containing aquifer. This is an interesting observation of a relationship between initial and trapped saturations. Whilst this fundamental rock phenomenon is routinely encountered in hydrocarbon recovery modelling (So<sub>i</sub> vs So<sub>r</sub> relationships for oil and Sg<sub>i</sub> vs Sg<sub>t</sub> [12] for gas), it is not typically thought of for water. However it is relevant in CO<sub>2</sub> storage scenarios when developing aquifer storage versus depleted gas field storage.

## 5.4 Comparison of keg at Sw<sub>i</sub> and keg at Sw<sub>r</sub> values and their use as endpoint values

The kr corefloods started from Sw=1. A keg at Sw<sub>r</sub> permeability of 64.2 mD was measured at the end of the high rate bump flood giving a kr relative to Sw=1 (112mD) of 0.53. This was measured at Sw<sub>r</sub>=0.43 PV after 80 PV of throughput.

At the start of the EGR the effective gas permeability was measured in the presence of a uniformly distributed Sw<sub>i</sub> of 0.12 PV. This keg at Sw<sub>i</sub> was measured at 163 mD, i.e.

significantly higher than  $k_{rg}$  at Swr. (As an aside, the reason why this  $k_{rg}$  at Swi is higher than the Sw=1 permeability has been suggested by some authors to be because the initial water saturation preferentially fills the smallest, most tortuous flow paths thereby creating a less tortuous flow path for the gas and termed the “lubricity” effect [24,25].)

Endpoint  $k_{rg}$  permeabilities are often calculated at the end of drainage coreflood tests as it is easy, convenient and seems intuitively correct to do so. However, a comparison of gas permeabilities at the end of the drainage floods in this study show they are invariably lower than those performed at the uniformly low initial water saturations achieved by desaturation using the porous plate method (As was done for the ambient floods and the EGR flood). Although this method represents a significantly more time-consuming preparation than commencing corefloods from Sw=1, it gives a gas permeability at a true residual water saturation which will be far more representative of the low water saturations found high in gas columns. These could be hydrocarbon gas in producing zones or at the top of geological structures used for CCS / CCUS after years of injection or plume migration.

## 6. Conclusions

A significant increase in CO<sub>2</sub> storage capacity was observed for secondary drainage into a representative paleo residual gas zone compared to primary drainage into an aquifer. The Swr to secondary drainage of 0.35 PV in the EGR test would also apply to areas of a depleted gas field where an active aquifer has advanced and trapped residual gas. For identical rock at the same conditions an Swr of 0.55 PV was found from primary drainage with CO<sub>2</sub> displacing brine.

When measuring  $S_{gt}(CO_2)$  for use in predicting capillary trapping storage for CCS / CCUS the use of correct fluids at reservoir conditions may be required for some rock types. The use of ambient condition model systems is attractive as it is quicker and easier but may give significantly optimistic CO<sub>2</sub> storage predictions.

This study aimed to test if concerns over whether a secondary drainage CO<sub>2</sub> flood would recover all trapped methane in a paleo residual gas zone were founded. In this case all CH<sub>4</sub> was recovered efficiently from a homogeneous rock. There was no evidence of significant water-blocking.

By combining results from the different corefloods in this study it is possible to provide a complete and representative set of relative permeability data and endpoint saturations for a CCUS development to be analysed in a reservoir simulation study. The paper also demonstrates some of the potential problems in using only simple experiments or model fluid systems to represent the complex fluid behaviours and interactions which may be encountered in CCUS developments.

This study has shown evidence which, although inconclusive, supports the hypothesis that CO<sub>2</sub> is partially wetting in the presence of brine in certain sandstone rocks. More work is required to understand why apparently inconsistent results have been found.

## Acknowledgments

The authors wish to acknowledge Debra Wells at Expro for useful discussions on GC analysis and rapid turnaround of data. Ambient condition coreflood tests were carried out by Mathew Hagger and reservoir condition corefloods by Chris Jones in BP's Production and Subsurface Laboratories in Sunbury. The petrographic study was run by Jon Crouch.

## References

1. IEA, Energy Technology Analysis; Prospects for CO<sub>2</sub> Capture and Storage, ISSN: 19901356 <https://doi.org/10.1787/19901356> (2004)
2. J. Underschultz, J Ennis- King et. al, International Journal of Greenhouse Gas Control, **5 Issue 4**, 922-932 (2011)
3. M. Burgt, J. Cantle, V. Boutkan, Energy Conversion and Management, **33**, 603-610 (1992)
4. K. Blok, R. Williams, R Katofsky, C. Hendriks, Energy, **22**, 161-168 (1997)
5. S. Melzer, “Stranded oil in the residual oil zone, U.S. Department of Energy, 91 (2006)
6. P. Bergmo, A Grimstad, K Kurtev, International Journal of Greenhouse Gas Control, **75**, 254-261 (2018)
7. B. Ren, I. Duncan, Journal of Petroleum Science and Engineering, **177**, 528-539 (2019)
8. H. Dennis, J. Ballie, T. Holt, D. Wessel-Berg, Norwegian Petroleum Society Special Publications, **9**, 171-185 (2000)
9. C. McPhee, J. Reed, I. Zubizarreta, Core Analysis: a Best Practice Guide, Elsevier (2015)
10. C.I. Nicholls, J. Heaviside, SPE Form Eval **3**, 01, 69-75 (1988) SPE-14421-PA
11. C. Jones, J. Brodie, M. Spearing, S. Lamb, Sadikoglu, K. E3S Web Conf. 89 01002 (2019)
12. C.S. Land, Soc. Pet. Eng. J., **8(2)**, 149-156 (1968).
13. E.F Johnson, D.P. Bossler, V.O.N. Bossler, SPE-1023-G, Pet. Trans. AIME, **216**, 370-372
14. F. Lomeland, E. Ebeltoft, W.H. Thomas, Proceedings of the 2005 International Symposium of the SCA (2005)
15. N.T. Burdine, Trans. Am. Inst. Min. Eng., **198**, 71-78 (1953)
16. G. Jerauld et al., Adipecc Proceedings SPE-188688-MS (2017)
17. S. Krevor, C Reynolds, Al-Menhali, Petrophysics, **57**, 12-18 (2016)
18. M. Fleury et.al, Energy Procedia, **4**, 5227-5234 (2011)
19. P. Chiquet, D. Broseta, S. Thibeau, SPE-94183-MS (2005)
20. Yang, D et.al, Energy & Fuels, **22(1)**, 504-509 (2008)
21. A.T. Grogan, W.V. Pinczewski, G.J. Ruskauff, F.M. Orr SPE Res. Eng. **3**, **01**, 93-102 (1988)
22. H.D. Do, W.V. Pinczewski, Chem Eng Sci, **48**, 3243-3252 (1993)

23. B. Bijeljic, A.H. Muggeridge, M.J. Blunt, Chem Eng Sci, **58**, 2377-2388 (2003)
24. C.A. McPhee, Advances in Petrophysics 95-97 (1994)
25. C.A. McPhee, K.G. Arthur, SPE 28826 199-211 (1994)